A Linear Multivariable Dynamical Model of a Supersonic Inlet-Engine Combination

Yanchen Guan,* Shin Yarng,† and Jiahnbo Yarng‡
Northwestern Polytechnical University, Xi'an, China

A linear multivariable dynamical model of a supersonic inlet-engine combination, which can be used for the integrated control design of the combination, is presented in both state space and frequency domain and its simulation. The inlet portion is modeled by applying and extending Willoh's method of inlet dynamical analysis with the piecewise lumped volumes of the subsonic duct to both the downstrem and upstream perturbation cases. The engine portion is primarily modeled on the linearized one-dimensional channel flow with the experimental data of the engine components considering variable specific heat of gas. The steady-state flow matching of the inlet and engine is carried out by varying the opening of the bypass doors. The stiff differential equations of the model are solved by the combined Newton-Raphson and Runge-Kutta methods with different time steps for different time intervals. Then, the dynamics of the inlet-engine combination is simulated digitally. The results from the simulation are compared with experimental data.

Nomenclature

A	= area, ft^2
a	= speed of sound, ft/s
AMP	= amplitude, dB
C	= coefficient
F	= thrust, lbf
j	= $\sqrt{-1}$
I	= compressor inlet guide vane angle, deg
K	= gain
L	= length, in.
M	= Mach number
N	= engine speed, rpm
P	= total pressure, psia
P_S	= static pressure, psia
PHA	= phase angle, deg
PR	= pressure recovery of inlet
s	= Laplace operator
T	= total temperature, °R
t	= time, s
Δt	= computation time step, s
v	= velocity, ft/s
W	= weight flow rate (air or fuel), lb/s
X	= any known value
Y	= displacement, in.
β	= oblique shock semiangle, deg
Δ	= disturbance, change, deviation
ζ	= damping ratio
θ,σ,τ	= transport time lag of inlet, s
$\mathbf{\Lambda}(s),\mathbf{\Phi}(s)$, $\mathbf{\Psi}(s),\mathbf{\Theta}(s)$	= Laplace transform of deviation vectors $\Delta\boldsymbol{R}(t)$, $\Delta\boldsymbol{U}(t)$, $\Delta\boldsymbol{X}(t)$, and $\Delta\boldsymbol{Z}(t)$
ρ	= specific gravity of air, lb/in^3
ϕ	= flow coefficient of inlet
$\psi(j\omega)$	= frequency response
ω	= frequency, Hz
$\boldsymbol{A},\boldsymbol{B}...\boldsymbol{L},\boldsymbol{O}$, $\boldsymbol{P},\boldsymbol{Q},\boldsymbol{\Gamma},\boldsymbol{\Pi}$	= matrices
$\boldsymbol{I}_0$	= unit matrix
$\boldsymbol{R},\boldsymbol{U},\boldsymbol{X},\boldsymbol{Z}$	= response, control, state, and disturbance vectors, respectively
$\boldsymbol{L}(s),\boldsymbol{V}(s)$	= transfer matrix of output deviation vector to control deviation vector $\Delta\boldsymbol{U}(t)$ and disturbance deviation vector $\Delta\boldsymbol{Z}(t)$

Superscripts

$(\bar{\ })$	= average value
$(\tilde{\ })$	= Laplace transform of nondimensional small perturbation
$(\dot{\ })$	= time derivative

Subscripts

$a,b,1,2,...,n,n+1,...$, CI,CD,T, N,E	= station number of the inlet-engine combination, Fig. 1a
B	= main burner
BP	= bypass
BL	= bleed
CD	= compressor discharge
CI	= compressor intake
E	= exit
EN	= engine
F	= fuel
FA	= afterburner fuel
GV	= inlet guide vane
H	= freestream
IEC	= inlet-engine combination
IN	= inlet
M	= metal
N	= nozzle
SP	= spike
SW	= normal shock wave
T	= turbine

Presented as Paper 84-1496 at the AIAA/SAE/ASME 20th Joint Propulsion Conference, Cincinnati, Ohio, June 11-13, 1984; received Nov. 8, 1984; revision received April 13, 1985.

*Professor, Department of Aero-Engine Engineering.
†Assistant Professor, Department of Aero-Engine Engineering.
‡Master's Degree Candidate, Department of Aero-Engine Engineering.

Introduction

FIGURE 1a is a cross-sectional view of a typical supersonic propulsion system of the inlet-engine combination. The inlet is an axisymmetric mixed-compression type with a translating centerbody and bypass door. The engine is a one-spool, multistage axial compressor with a variable inlet guide

vane and bleeding doors, and afterburning with a variable exhaust nozzle.

An integrated control system is required not only to provide optimum overall propulsion performance but to provide operational reliability and safety as well. Evidently, design of such a high-performance, multivariable control system requires a mathematical dynamical model of the inlet-engine combination as an integrated control object. The purpose of this paper is to develop such a linear multivariable model for integrated control design.

Inlet and engine dynamics have been analyzed and modeled in a number of ways in the available literature. For example, Fraiser,[1] Mays,[2] Willoh,[3] and Cole and Willoh[4] have presented different inlet dynamical models. Seldner et al.,[5] Stone et al.,[6] Miller and Hackney,[7] and Geyser,[8] and Guan and Zhang[9] have presented dynamical models for different engine types. On the other hand, publications on the subject of mathematical modeling of integrated inlet-engine combinations are few, although development and research work on integrated propulsion control systems has been underway in many countries over the past 10 years. Chun and Swanson[10] have presented analog simulation of an inlet-engine combination and Wasserbauser[11] has completed an experimental investigation on dynamical response of an inlet-engine combination. Beattie[12] has presented a design of a multivariable integrated control for a supersonic propulsion system, but has not given the mathematical formulation. The purpose of this paper is to develop such a model.

Mathematical Modeling

Formulation of the Problem

The multivariable nonlinear dynamical behavior of the inlet-engine combination shown in Fig. 1 can be described by the state equation

$$\dot{X}=f(X,U,Z) \tag{1}$$

and the output equation

$$R=h(X,U,Z) \tag{2}$$

where

$X=[Y_{SW},N,T_M,T_N]^T$ 4×1 vector

$U=[A_{BP},Y_{SP},I_{GV},A_{BL},W_F,W_{FA},A_E]^T$ 7×1 vector

$Z=[M_H,P_{SH},T_{SH}]^T$ 3×1 vector

$R=[Y_{SW},P_{S1},P_{S2},N,P_{CD},W_{EN},T_B,T_T,P_T,F]^T$ 10×1 vector

These state, control, and output variables are selected according to the actual construction, effectiveness to the control, convenience of measurement, and simplification of unnecessary complexity of the control system.

While its linear multivariable dynamical model can be described by

$$\Delta\dot{X}=A\Delta X+B\Delta U+G\Delta Z \tag{3}$$

$$\Delta R=C\Delta X+D\Delta U+H\Delta Z \tag{4}$$

where A, B, C, D, G, and H are Jacobian matrices of dynamical coefficients of the plant and ΔX, ΔU, ΔZ, and ΔR are deviation vectors of state, control, disturbance, and output variables, respectively.

Derivation of Eqs. (3) and (4) is presented in the Appendix.

Realization of the Model

In ordinary speed and temperature control system, only low-frequency dynamics of the engine is required, while the high-frequency factors, such as gas compressibility, energy storage, and transport lags in components, are neglected. Therefore, the low-frequency model of the engine is directly developed in the time domain without difficulty. Willoh's model of inlet dynamics has been presented primarily based upon linearized distributed parameter wave equations in the frequency domain by a closed-form matrix solution with piecewise lumped volumes of a subsonic duct in order to reduce the complexity of mathematical computation. Therefore, the method of modeling of the inlet-engine combination presented herein is such that 1) the inlet is modeled in the frequency domain by applying and extending Willoh's method and the engine is modeled in the time domain separately at first; 2) the inlet and engine are flow-matched in steady state by bypassing the excess airflow; 3) at the matching point, the linearized dynamical model of the inlet is transformed into the form of the time domain; and 4) the inlet and engine models are matched dynamically at the steady-state matching point as the initial point of a transient process. State-space and frequency models of the integrated combination can be computed from the dynamically matched separate models of the inlet and engine.

Inlet Dynamical Model (Frequency Domain)[13]

For a quasi-one-dimensional flow with the assumptions of perfect gas relations, a constant specific heat ratio of 1.4 and inviscid-nonheat-conducting fluid, applying Willoh's method, the inlet dynamics can be developed as:

Normal shock position to the bypass transfer function:

$$\frac{\tilde{Y}_{SW}(s)}{\tilde{A}_{BP}(s)}=\frac{PE_{E-1}(s)\ldots E_{n+1}(s)I_2}{PE_{E-1}(s)\ldots E_{n+1}(s)\ldots E_2(s)Q(s)} \tag{5}$$

Normal shock position to the freestream disturbance transfer functions:

$$\frac{\tilde{Y}_{SW}(s)}{\tilde{P}_{SH}(s)}=-\Gamma(s)K_1L_bL_aI_1 \tag{6}$$

$$\frac{\tilde{Y}_{SW}(s)}{\tilde{T}_{SH}(s)}=-\Gamma(s)K_1L_bL_aI_2 \tag{7}$$

$$\frac{\tilde{Y}_{SW}(s)}{\tilde{M}_H(s)}=-\Gamma(s)K_1L_bL_aI_3 \tag{8}$$

Normal shock position to the spike position transfer function:

$$\frac{\tilde{Y}_{SW}(s)}{\tilde{Y}_{SP}(s)}=-\Gamma(s)f_{SP}(Y_{SP})I_2 \tag{9}$$

Static pressure behind the normal shock to the bypass transfer function:

$$\frac{\tilde{P}_{S2}(s)}{\tilde{A}_{BP}(s)}=\Pi Q(s)\frac{\tilde{Y}_{SW}(s)}{\tilde{A}_{BP}(s)} \tag{10}$$

Other transfer functions of required parameters can be deducted from gas relations.

The detailed expressions of matrices P, E_{E-1}, ... in Eqs. (5-10) can be found in Ref. 13.

Engine Model (Time Domain)

The nonlinear steady-state and dynamical models of the engine represented by Eqs. (A6) and (A7) are developed by using Seldner's generalized simulation technique, and the state-space model of the engine [Eqs. (A8) and (A9)] is then obtained by the linearization method. Newton-Raphson's multivariable iteration method of solving simultaneous

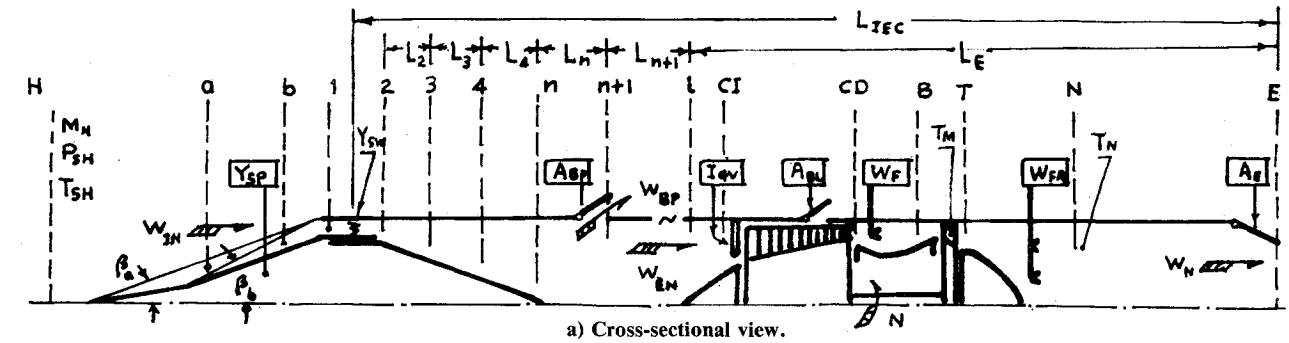

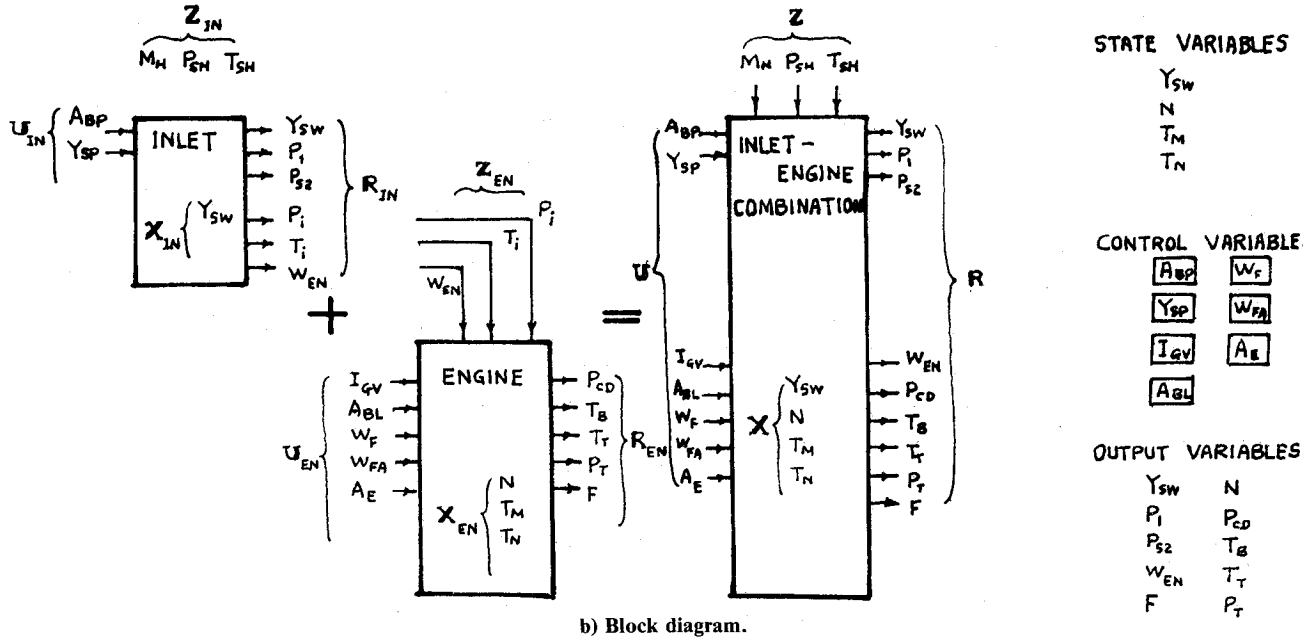

Fig. 1 Inlet-engine combination.

nonlinear equations and Runge-Kutta's method of solving ordinary differential equations are used.

Steady-State Flow Matching of Inlet and Engine

Under a definite flight condition, the flow matching of the inlet and engine is performed by bypassing the excess portion of air entering the inlet to attain critical operation. Thus, at this matching point, the air supplied by the inlet is equal to the air demanded by the engine, or

$$W_{IN} - W_{BP} = W_{EN} \tag{11}$$

The airflow rate of the inlet W_{IN} can be calculated by (refer to Fig. 1a)

$$W_{IN} = \rho_H A_H v_H \phi_{IN} \tag{12}$$

and the flow coefficient of the inlet ϕ_{IN} can be interpolated from the inlet stedy-state characteristics (Fig. 2) for a given flight condition.

The airflow rate of the engine W_{EN} for a given intake condition of P_i, T_i and given speed N can be computed directly from the engine model at the matching point. Equilibrium of total pressure P_i and airflow rate W_{EN} can be established by successive iterations.

Dynamical Matching of the Inlet and Engine

The steady-state matching point is then selected as the initial point of dynamical matching of the combination.

Frequency Response of the Inlet

Frequency response of the inlet can be calculated by replacing the Laplace transform operator s of each element in the matrices of Eq. (5-10) with $j\omega$. For example, from Eq. (5), we can get frequency response of the normal shock position to bypass

$$\frac{\tilde{Y}_{SW}(j\omega)}{\tilde{A}_{BP}(j\omega)} = \psi(j\omega) = \psi_{Re}(\omega) + j\psi_{Im}(\omega) \tag{13}$$

where ψ_{Re} and $\psi_{Im}(\omega)$ are the real and imaginary parts of the frequency response, respectively.

Time Response of the Inlet

From control theory, the unit step response $g(t)$ of a system can be transformed from its frequency response by the relation

$$g(t) = \frac{2}{\pi}\int_0^\infty \frac{\psi_{Re}(\omega)}{\omega}\sin\omega t d\omega \tag{14}$$

State-Space Model of the Inlet

The transfer functions of Eqs. (5-10) contain delay-time terms $e^{\tau_1 s}$, $e^{-\sigma_1 s}$, $e^{-\theta_1 s}$,..., that have an infinite number of poles and from which our intent is to develop a finite-order state variable formation of the inlet. Therefore, Eqs. (5-10) must be modified and can be approximated using curve fitting

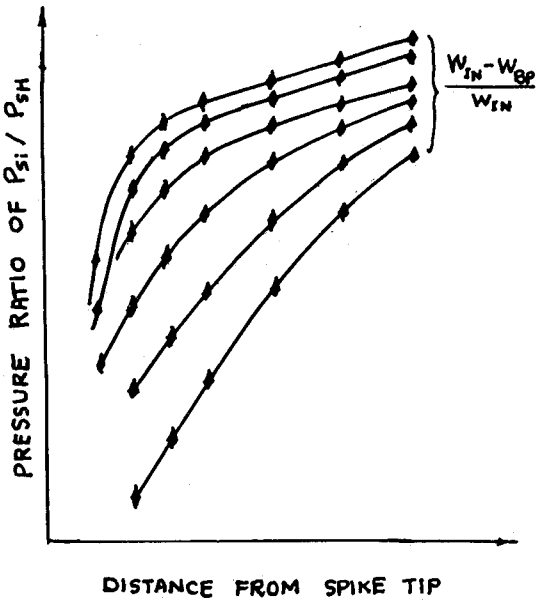

Fig. 2 Steady-state characteristics of inlet.

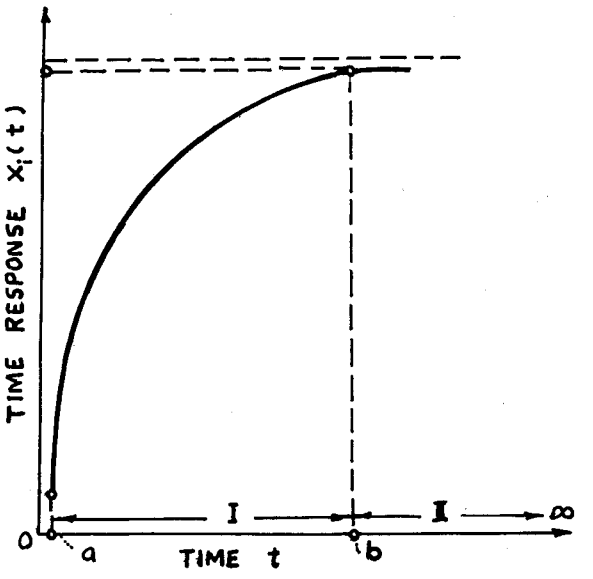

Fig. 3 Time response curve.

method[14] into the standard form

$$K\left(\frac{s}{\omega_1}+1\right)\left(\frac{s}{\omega_2}+1\right)\cdots\left(\frac{s^2}{\omega_m^2}+\frac{2\zeta_m s}{\omega_m}+1\right)\times\left(\frac{s^2}{\omega_{m+1}^2}+\frac{2\zeta_{m+1}s}{\omega_{m+1}}+1\right)\cdots\Big/\left[s^p\left(\frac{s}{\omega_j}+1\right)\times\left(\frac{s}{\omega_{j+1}}+1\right)\cdots\left(\frac{s^2}{\omega_n^2}+\frac{2\zeta_n s}{\omega_n}+1\right)\times\left(\frac{s^2}{\omega_{n+1}^2}+\frac{2\zeta_{n+1}s}{\omega_{n+1}}+1\right)\cdots\right] \tag{15}$$

where ζ_m, ζ_{m+1}, ζ_n, ζ_{n+1}, ..., are damping ratios; ω_m, ω_{m+1}, ..., ω_j, ω_{j+1}, ..., ω_n, ω_{n+1}, ..., are frequencies; p the number of integral elements; and K the gross system gain.

Then the frequency-domain representation of Eq. (15) can be transformed into the state-space form of Eqs. (A3) and (A4) using the phase variable transformation.[15]

Time Response of the Inlet-Engine Combination

Now, setting a step ramp of each control variable (such as bypass area A_{BP} or fuel flow rate W_F) successively to the combination model [Eqs. (A3), (A4), (A6) and (A7)], transient responses of state and output variables can be calculated simultaneously by digital simulation of the model.

Frequency Response of the Inlet-Engine Combination

From the Laplace transform relation

$$X_i(j\omega)=\int_0^\infty X_i(t)e^{-j\omega t}dt \tag{16}$$

for a given time-response curve (Fig. 3), the integral interval of time may be divided into [O, a], [a, b] and [b, O] as shown. Point a is selected near the origin O but not equal to zero to avoid overflow in the process of digital computation. Point b is on the asymptote of the new steady-state condition.

In the interval [O, a]

$$X_i(t)=0$$

Hence,

$$X_i(j\omega)\doteq X_{i1}(j\omega)+X_{i2}(j\omega)=\int_a^b X_i(t)e^{-j\omega t}+\int_b^\infty X_i(t)e^{-j\omega t}dt \tag{17}$$

Since $X_i(t)$ and time t had been given in discrete data value, the first term of the above equation can be computed by Simpson's method of integration, and the second term can be computed as

$$\begin{aligned}X_{i2}(j\omega)&=\int_b^\infty X_i(t)e^{-j\omega t}dt\\&=\int_b^\infty X_i(I)e^{-j\omega t}dt\\&=X_i(I)e^{-j\omega b}/j\omega\end{aligned} \tag{18}$$

where $X_i(I)$ is the known value of the response $X_i(t)$ at time b.

State-Space Model of the Inlet-Engine Combination

Equations (3) and (4) can be computed from the time response of the combination by the method of linearization or by combining the state-space models of the inlet and engine into partitioned matrix form as shown in the Appendix.

Digital Simulation Results

Figure 4 shows the flowchart of the program.

For an example of the computation, the NASA 48-cm axisymmetric mixed-compression-type inlet (having 60% internal supersonic area contraction at the design Mach number 2.5, capture area of 272.8 in.^{2}, and a design-corrected airflow of 35.7 lb/s, and the J85-13 turbojet engine (with rated speed of 16,500 rpm, rated airflow of 44.2 lb/s, and rated dry thrust of 2296 (lbf) were selected. Their steady-state performance characteristics are taken from Refs. 16 and 17.

It is found that the time constant of the inlet is approximately 0.02-0.05s and the time constants of the engine (rotor dynamics and thermodynamics of turbine materials) are approximately 1 s. Hence, the inlet-engine combination dynamics is a set of stiff differential equations with a degree of stiffness

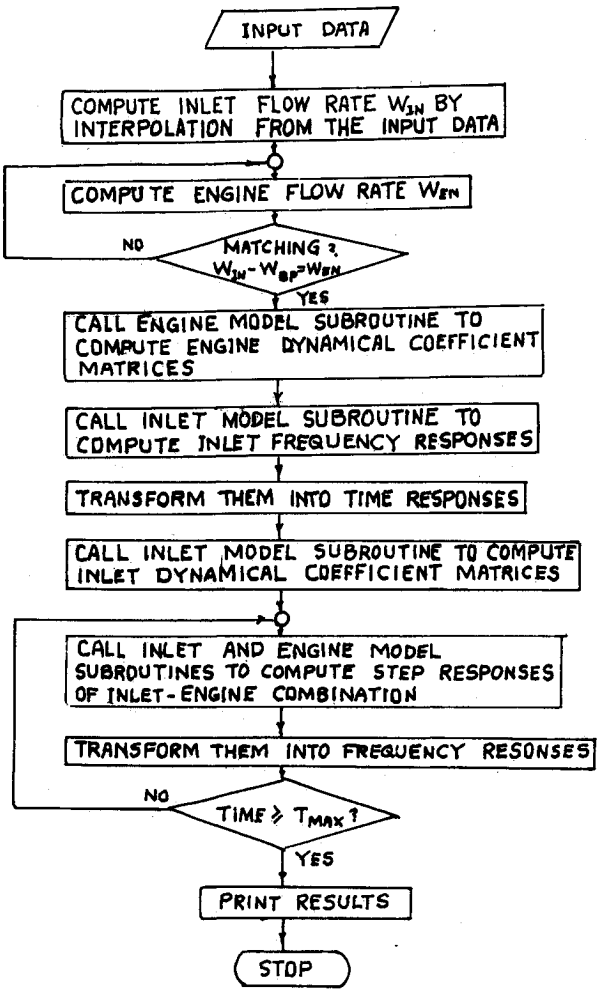

Fig. 4 Flowchart of digital simulation.

around 10^2. These stiff equations are solved by combining the Newton-Raphson and Runge-Kutta methods with different time steps for different time intervals. In the first 0.02 s time interval, a time step of 0.001 s is taken to compute the responses of inlet alone without considering the effect of engine dynamics on inlet responses. Thereafter, at the time interval of 0.02 s and after, the inlet and engine are dynamically matched using a time step of 0.025 s.

Figures 5-7 show the typical responses of the state and output variables to the control of bypass at a flight condition of Mach number 2.46, total temperature of 702°R, total pressure of 15.5 lb/in.^{2}, and engine speed of 16,170 rpm.

Transient Responses

Figure 5 shows the responses of the normal shock position Y_{SW}, static pressure behind the normal shock P_{S2}, static exit pressure of the inlet P_{Si}, flow rate of the engine W_{EN}, total inlet temperature of the turbine T_B, total compressor discharge pressure P_{CD}, engine speed N, and thrust F of the combination to a 3% step increase in bypass air (or 1.12 lb/s).

The normal shock position and related inlet variables P_{S2} and P_{Si} are increased to their new steady value quickly in 0.05 s and oscillated periodically with a small amplitude, while the engine flow rate W_{EN} is decreased to a new steady value quickly in 0.02 s. These responses represent the high-frequency nature of gas compressibility and the high traveling speed of a small air disturbance.

The engine speed N and its related variable P_{CD} are increased monotonically to the new steady value slowly in 3.0 s with a slight oscillation. This reflects the low-frequency nature of a large moment of inertia of the engine rotor. The thust F is suddenly decreased much below its original steady value due to a sudden decrease in the engine flow rate W_{EN} and increased gradually to a value higher than its original steady value due to the increase of engine speed N.

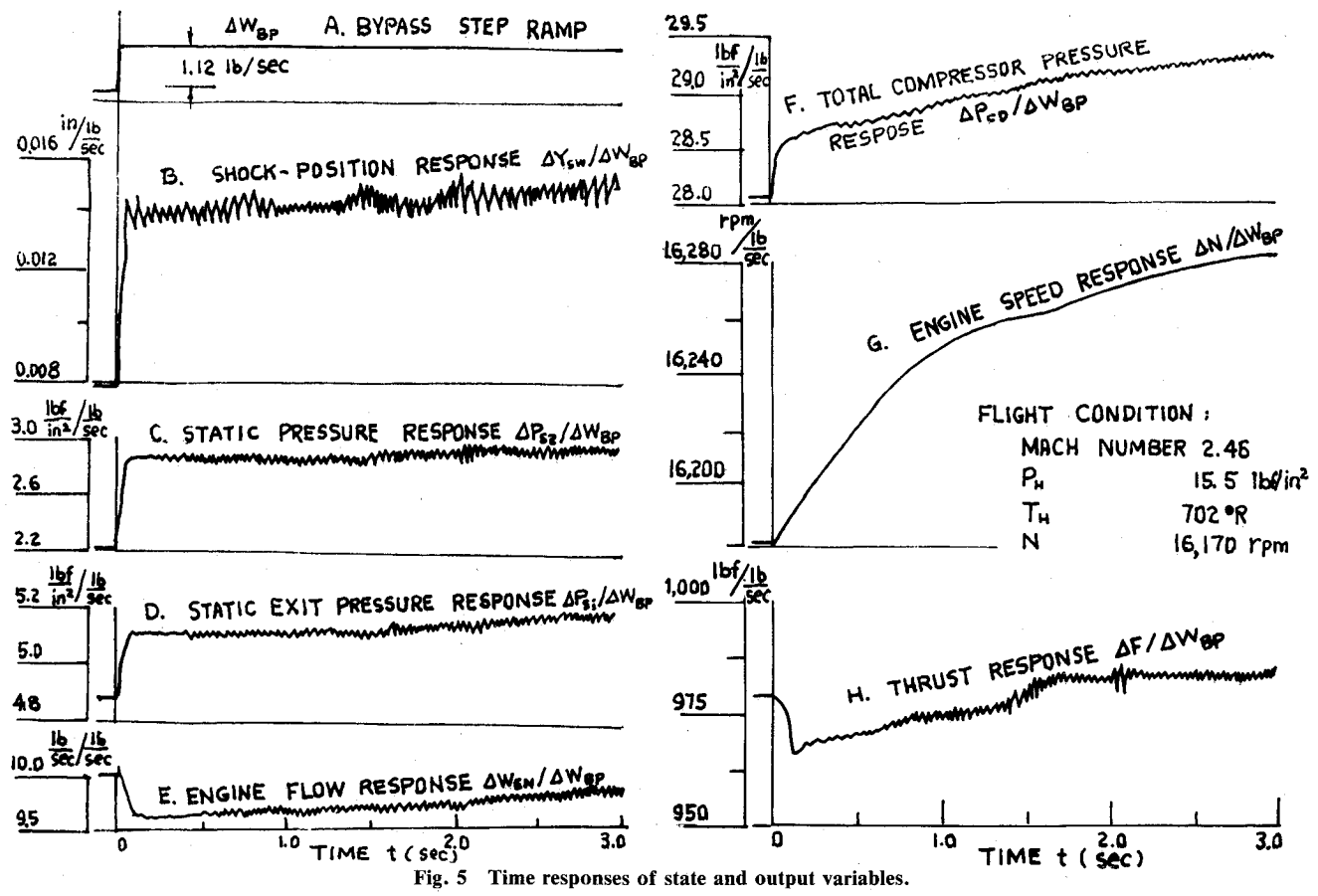

Fig. 5 Time responses of state and output variables.

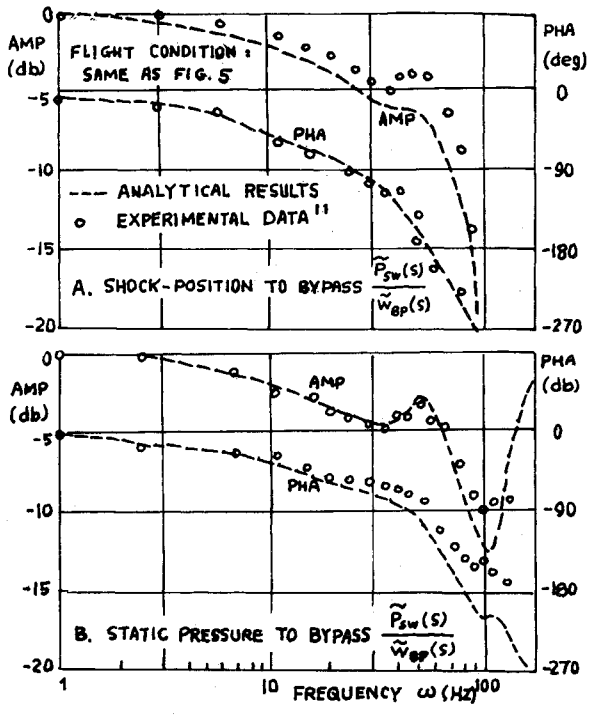

Fig. 6 Frequency responses.

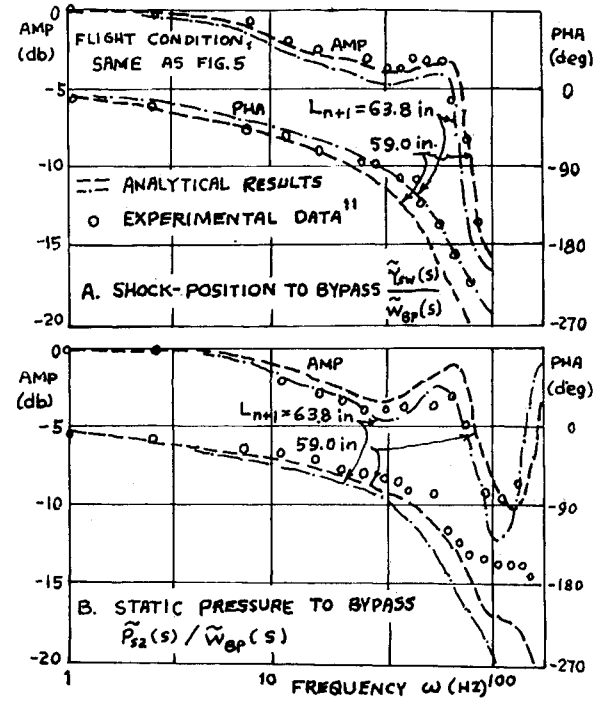

Fig. 7 Effect of length of inlet extension duct.

Frequency Responses and Experimental Verification

The analytical frequency responses of normal shock position Y_{SW} and static pressure P_{S2} to the bypass flow of the combination are given by the solid lines of Figs. 6 and 7, while the data points of Figs. 6 and 7 show the corresponding experimental frequency responses. It can be seen that they are quite agreeable when lower than 30 Hz and relatively discrepant when higher than 40 Hz.

Effect of Inlet Extention Duct Length

Figure 7 shows the effect of the length of the inlet extension duct (L_{n+1} in Fig. 1a) on the dynamical behavior of the inlet. It can be seen that the response frequency will be decreased by increasing the length of the extension duct. This represents an increase in the gas capacity of the duct.

Concluding Remarks

A mathematical method of modeling the linear multivariable dynamical behavior of the supersonic inlet-engine combination and its digital simulation both in the frequency and time domains was presented. The results of the method were found to be in quite good agreement with experimental data below 30 Hz, but not as good above 40 Hz; probably due to the imperfection of the one-dimensional gas flow modeling of the inlet due to many factors, e.g., boundary-layer influences, flow distortion, and actual two- or three-dimensional phenomena had not been considered.

In general, the method developed herein can be applied to other types of inlet-engine combinations. Further work is required to refine this model.

Appendix

Derivation of State-Space Model of the Inlet-Engine Combination

For convenience of analysis and computation, the mathematical model can be formulated in the inlet and engine separately at first and then integrated into one.

State-Space Model of the Inlet

As shown in Fig. 1b, the nonlinear dynamical behavior of the inlet can be described by the state equation

$$\dot{X}_{IN} = f_{IN}(X_{IN}, U_{IN}, Z_{IN}) \tag{A1}$$

output equation

$$R_{IN} = h_{IN}(X_{IN}, U_{IN}, Z_{IN}) \tag{A2}$$

where

$X_{IN} = [X_1, X_2, \ldots X_p]^T$ $p \times 1$ vector, composed of variable $Y_{SW}, \ldots$

$U_{IN} = [U_1, U_2, \ldots U_q]^T$ $q \times 1$ vector, composed of variable A_{BP}, $Y_{SW}, \ldots$

$Z_{IN} = [Z_1, Z_2, \ldots Z_r]^T$ $r \times 1$ vector, composed of variable M_H, $P_{SH}, T_{SH}, \ldots$

$R_{IN} = [R_1, R_2, \ldots R_S]^T$ $s \times 1$ vector, composed of variable Y_{SW}, P_{S2}, P_{Si}, T_i, $W_{EN}, \ldots$

are in more generalized form. Let

$$f_{IN}(X_{IN}, U_{IN}, Z_{IN}) = [f_1, f_2, \ldots f_p]^T$$

$$h_{IN}(X_{IN}, U_{IN}, Z_{IN}) = [h_1, h_2, \ldots h_s]^T$$

then the linear dynamical model of the inlet can be developed by Taylor's series expansion at a particular operating point as

$$\Delta\dot{X}_{IN} = A_{IN}\Delta X_{IN} + B_{IN}\Delta U_{IN} + G_{IN}\Delta Z_{IN} \tag{A3}$$

$$\Delta R_{IN} = C_{IN}\Delta X_{IN} + D_{IN}\Delta U_{IN} + H_{IN}\Delta Z_{IN} \tag{A4}$$

where A_{IN}, B_{IN}, G_{IN}, C_{IN}, D_{IN}, and H_{IN} are $p \times p$, $p \times q$, $p \times r$, $s \times p$, $s \times q$, and $s \times r$ Jacobian coefficient matrices of the inlet and matrices C_{IN}, D_{IN}, and H_{IN} may be rewritten as partitioned forms as

$$C_{IN} = \begin{bmatrix} C_{IN,1} \\ \hline C_{IN,2} \end{bmatrix} \quad D_{IN} = \begin{bmatrix} D_{IN,1} \\ \hline D_{IN,2} \end{bmatrix} \quad H_{IN} = \begin{bmatrix} H_{IN,1} \\ \hline H_{IN,2} \end{bmatrix}$$

where $C_{IN,1}$, $C_{IN,2}$, $D_{IN,1}$, $D_{IN,2}$, $H_{IN,1}$, and $H_{IN,2}$ are $p\times p$, $(s-p)\times p$, $q\times q$, $(s-q)\times q$, $r\times r$, $(s-r)\times r$ matrices.

And

$$\Delta X_{IN} = [\Delta X_1, \Delta X_2, \ldots \Delta X_p]^T$$

$$\Delta U_{IN} = [\Delta U_1, \Delta U_2, \ldots \Delta U_q]^T$$

$$\Delta Z_{IN} = [\Delta Z_1, \Delta Z_2, \ldots \Delta Z_r]^T$$

$$\Delta R_{IN} = [\Delta R_1, \Delta R_2, \ldots \Delta R_s]^T = \begin{bmatrix} \Delta R_{IN,1} \\ \hline \Delta R_{IN,2} \end{bmatrix}$$

where $\Delta R_{IN,1}$ and $\Delta R_{IN,2}$ are $p\times 1$ and $(s-p)\times 1$ matrices.

Equation (A4) may be rewritten as

$$\Delta R_{IN} = \begin{bmatrix} \Delta R_{IN,1} \\ \hline \Delta R_{IN,2} \end{bmatrix} = \begin{bmatrix} C_{IN,1} \\ \hline C_{IN,2} \end{bmatrix} \Delta X_{IN} + \begin{bmatrix} D_{IN,1} \\ \hline D_{IN,1} \end{bmatrix} \Delta U_{IN} + \begin{bmatrix} H_{IN,1} \\ \hline H_{IN,2} \end{bmatrix} \Delta Z_{IN} \tag{A5}$$

State-Space Model of the Engine

In the same manner, the nonlinear dynamical behavior of the engine can be described by

$$\dot{X}_{EN} = f_{EN}(X_{EN}, U_{EN}, Z_{EN}) \tag{A6}$$

$$R_{EN} = h_{EN}(X_{EN}, U_{EN}, Z_{EN}) \tag{A7}$$

where

$X_{EN} = [X_{p+1}, X_{p+2}, \ldots X_t]^T$ $(t-p)\times 1$ vector, composed of variables N, T_M, T_N, ...

$U_{EN} = [U_{q+1}, U_{q+2}, \ldots U_u]^T$ $(u-q)\times 1$ vector, composed of variables I_{GV}, A_{BL}, W_F, W_{FA}, A_E, ...

$Z_{EN} = [Z_{r+1}, Z_{r+2}, Z_3]^T$ $(s-p)\times 1$ or 3×1 vector, composed of variables P_{Si}, T_i, W_{EN}

$= R_{IN,2}$

$R_{EN} = [R_{S+1}, R_{S+2}, \ldots R_w]^T$ $(w-s)\times 1$ vector, composed of variables P_{CD}, T_B, T_T, P_T, F, ...

and the linear dynamical model of the engine can be written as

$$\Delta \dot{X}_{EN} = A_{EN}\Delta X_{EN} + B_{EN}\Delta U_{EN} + G_{EN}\Delta Z_{EN} \tag{A8}$$

$$\Delta R_{EN} = C_{EN}\Delta X_{EN} + D_{EN}\Delta U_{EN} + H_{EN}\Delta Z_{EN} \tag{A9}$$

where A_{EN}, B_{EN}, G_{EN}, C_{EN}, D_{EN}, H_{EN}, ΔX_{EN}, ΔU_{EN}, ΔZ_{EN}, and ΔR_{EN} are $(t-p)\times(t-p)$, $(t-p)\times(u-q)$, $(t-p)\times 3$, $(w-s)\times(t-p)$, $(w-s)\times(u-q)$, $(w-s)\times 3$, $(t-p)\times 1$, $(u-q)\times 1$, 3×1, and $(w-s)\times 1$ matrices, respectively.

State-Space Model of the Inlet-Engine Combination

Combining Eqs. (A3) and (A5) with Eqs. (A8) and (A9), we have the state-space model of the inlet-engine combination of Eqs. (3) and (4), where

$$\Delta X = \begin{bmatrix} \Delta X_{IN} \\ \hline \Delta X_{EN} \end{bmatrix} t\times 1 \text{ vector} \qquad \Delta U = \begin{bmatrix} \Delta U_{IN} \\ \hline \Delta U_{EN} \end{bmatrix} u\times 1 \text{ vector}$$

$$\Delta Z = \Delta Z_{IN} \quad v\times 1 \text{ vector} \qquad \Delta X = \begin{bmatrix} \Delta R_{IN,1} \\ \hline \Delta R_{EN} \end{bmatrix} w\times 1 \text{ vector}$$

$$A = \begin{bmatrix} A_{IN} & 0 \\ \hline G_{EN}G_{IN} & A_{EN} \end{bmatrix} (t\times t) \qquad B = \begin{bmatrix} B_{IN} & 0 \\ \hline G_{EN}D_{IN,2} & D_{EN} \end{bmatrix} (t\times u)$$

$$C = \begin{bmatrix} C_{IN,1} & 0 \\ \hline H_{EN}C_{IN,2} & C_{EN} \end{bmatrix} (w\times t) \qquad D = \begin{bmatrix} D_{IN,1} & 0 \\ \hline H_{EN}D_{IN,2} & B_{EN} \end{bmatrix} (w\times v)$$

$$G = \begin{bmatrix} G_{IN} \\ \hline G_{EN}H_{IN,2} \end{bmatrix} (t\times v) \qquad H = \begin{bmatrix} H_{IN,1} \\ \hline H_{EN}H_{IN,2} \end{bmatrix} (w\times v)$$

Derivation of Frequency-Domain Model of the Inlet-Engine Combination

The vectors and matrices in Eqs. (1) and (2) all are functions of time, thus

$$\Delta \dot{X}(t) = A\Delta X(t) + B\Delta U(t) + G\Delta Z(t) \tag{A10}$$

$$\Delta R(t) = C\Delta X(t) + D\Delta U(t) + H\Delta Z(t) \tag{A11}$$

for a zero initial condition, may be rewritten in the form of a Laplace transform as

$$s\Psi(s) = A\Psi(s) + B\Phi(s) + G\Theta(s) \tag{A12}$$

$$\Lambda(s) = C\Psi(s) + D\Phi(s) + H\Theta(s) \tag{A13}$$

Equation (A12) may be rewritten as

$$(sI_0 - A)\Psi(s) = B\Phi(s) + G\Theta(s) \tag{A14}$$

$$\Psi(s) = (sI_0 - A)^{-1}[B\Phi(s) + G\Theta(s)] \tag{A15}$$

or

$$(sT_0 + I_0)\Psi(s) = K_u\Phi(s) + K_z\Theta(s) \tag{A16}$$

where

$T = (-A)^{-1}$	time constant matrix
$K_u = (-A)_B^{-1}$	gain matrix of state vector to control vector
$K_z = (-A)_G^{-1}$	gain matrix of state vector to disturbance vector

Substituting Eq. (A15) into Eq. (A13) and rearranging, we have

$$\Lambda(s) = C[sI_0 - A]^{-1}[B\Phi(s) + G\Theta(s)] + D\Phi(s) + H\Theta(s)$$

$$= L(s)\Phi(s) + V(s)\Theta(s) \tag{A17}$$

where

$$L(s) = C[sI_0 - A]^{-1}B + D$$

$$V(s) = C[sI_0 - A]^{-1}G + H$$

Therefore, Eqs. (A16) and (A17) represent the mathematical model of the inlet-engine combination in the frequency domain.

References

[1]Fraiser, H. R., "Supersonic Inlet Dynamics," *Journal of the Aeronautical Sciences*, Vol. 27, 1960, pp. 429-436.

[2]Mays, R. A., "Inlet Dynamics and Compressor Surge," *Journal of Aircraft*, Vol. 18, April 1971, pp. 219-226.

[3]Willoh, R. G., "A Mathematical Analysis of Supersonic Inlet Dynamics," NASA TN D-4969, 1968.

[4]Cole, G. and Willoh, R., "Analysis of the Dynamic Response of a Supersonic Inlet to Flow Field Perturbations Upstream of the Normal Shock," NASA TN D-7839, 1975.

[5]Seldner, K., Mihaloew, J. R., and Blaha, R. J., "Generalized Simulation Technique for Turbojet Engine System Analyses," NASA TN D-6610, 1972.

[6]Stone, C. R., Miller, N. E., and Ward, M. D., "Turbine Engine Control Synthesis," Vols. I and II, AFAPL-TR-75-14, 1975.

[7]Miller, R. J. and Hackney, R. D., "F100 Multivarible Control System Engine Models/Design Criteria," AFAPL-TR-76-74 (AD A033532), 1976.

[8]Geyser, L. C., "DYGABCD—A Program for Calculating Linear A, B, C and D Matrices from a Nonlinear Dynamic Engine Simulation," NASA TP 1295, 1978.

[9]Guan, Y. S. and Zhang, S. X., "Mathematical Model of the Aircraft Gas Turbine Engine and Its Digital Simulation," Northwestern Polytechnical University, Xi'an, China 1982, (in Chinese).

[10]Chun, K. S. and Swanson, D. S., "Simulation of Supersonic Inlet and Engine," AIAA Paper 64-598, 1964.

[11]Wasserbauser, J. F., "Dynamic Response of a Mach 2.5 Axisymmetric Inlet with Engine or Cold Pipe and Utilizing 60% Supersonic Internal Area Contraction," NASA TN-5338, 1969.

[12]Beattie, E. C., "Design of a Multivariable Integrated Control for a Supersonic Propulsion System," NASA CP-2137, 1979.

[13]Yarng, S., "Mathematical Model of Supersonic Inlet and Its Digital Simulation," M.E. Thesis, Northwestern Polytechnical University, Xi'an, China, Jan. 1983 (in Chinese).

[14]Yarng, S., "A Method of Average Weighted Performance Function of Curve Fitting to Identify Transfer Function from Frequency Response," Northwestern Polytechnical University, Xi'an, China, Feb. 1984 (in Chinese).

[15]Schultz, D. G., *State Functions and Linear Control Systems*, McGraw-Hill Book Co., New York, 1967.

[16]Cubbison, R. W., Meleason, E. T., and Johnson, D. F., "Performance Characteristics from Mach 2.58 to 1.98 of an Axisymmetric, Mixed-Compression Inlet System with 60-Percent Internal Contraction," NASA TM X-1739, 1969.

[17]Antl, T. J. and Burley, R. R., "Steady State Airflow and Afterburning Performance Characteristics of Four J85-GE-13 Turbojet Engines," NASA TM X-1742, 1970.